Available online at www.sciencedirect.com
SCIENCE DIRECT®
Journal of Solid State Chemistry 177 (2004) 3934–3938
JOURNAL OF SOLID STATE CHEMISTRY
www.elsevier.com/locate/jssc

Single crystal growth, crystal structure characterization and magnetic properties of $UCo_{0.5}Sb_2$

Z. Bukowski*, V.H. Tran, J. Stepień-Damm, R. Troć

W. Trzebiatowski Institute of Low Temperature and Structure Research, Polish Academy of Sciences, P.O. Box 1410, 50-950 Wrocław, Poland

Received 9 June 2004; received in revised form 28 July 2004; accepted 2 August 2004
Available online 18 September 2004

Abstract

Single crystals of uranium intermetallic compound $UCo_{0.5}Sb_2$ were grown by means of the antimony-flux technique. The characterization of the samples has been carried out utilizing single crystal X-ray diffraction and magnetization measurements. $UCo_{0.5}Sb_2$ is found to crystallize in the tetragonal $HfCuSi_2$-type structure, space group $P4/nmm$ with $Z = 2$ formula units per cell, and the lattice parameters $a = 0.4300(1)$ and $c = 0.8958(2)$ nm. The refinement of the occupancy parameters and the energy dispersive X-ray analysis have indicated a distinct deficiency on the cobalt sites. The results of magnetization measurements showed that $UCo_{0.5}Sb_2$ orders ferromagnetically below 65 K with a huge magnetocrystalline anisotropy with the c direction being the easy magnetization axis.

PACS: 71.20.Lp; 75.30.Gw; 81.10.−h

Keywords: Single crystal; Ferromagnetic ordering; Magnetocrystalline anisotropy

1. Introduction

The intermetallic compounds $UTSb_2$ (T = Ru, Fe, Co, Ni, Pd, Cu, Ag and Au) were reported by Kaczorowski et al. [1] to crystallize in the tetragonal $HfCuSi_2$-type structure (space group $P4/nmm$) [1,2]. This series of compounds presents an interesting evolution in the magnetic properties, ranging from a paramagnetic ($UFeSb_2$), antiferromagnetic ($UTSb_2$, T = Ru, Ni and Pd) to a ferromagnetic (T = Cu, Ag and Au) ordering [1]. Moreover, on the basis of the temperature dependence of electrical resistivity a Kondo lattice-like behavior has also been suggested. These findings encourage us to perform further investigations, especially, in order to gain information on the anisotropy of the physical properties. Since the data known so far have been collected on poly-crystalline samples only, we have initiated an extended program of growing single crystals of the $UTSb_2$ compounds.

Recently we have grown and studied $UNi_{0.5}Sb_2$ single crystals [3] and now we report on the single crystal growth and characterization of $UCoSb_2$. Although the existence of stoichiometric $UCoSb_2$ has been already reported [1], its magnetic properties have not been recognized because of the sample contamination with traces of unreacted Co. The single crystals obtained by us were completely free of metallic Co or other ferromagnetic impurities. In contrast to the poly-crystalline samples, our single crystals appeared to be Co-deficient with the estimated composition of $UCo_{0.5}Sb_2$. Their good quality and sufficient size make it possible to determine the physical properties of this compound, for the first time. We will show here that $UCo_{0.5}Sb_2$ is a ferromagnet below 65 K with the c-axis being the magnetization easy axis and exhibiting a huge magnetocrystalline anisotropy. We tentatively interpret this anisotropy as arising due to an anisotropic hybridization between the $5f$—and ligand electrons.

*Corresponding author. Fax: +48-71-3441029.
E-mail address: bukowski@int.pan.wroc.pl (Z. Bukowski).

0022-4596/$ - see front matter © 2004 Elsevier Inc. All rights reserved.
doi:10.1016/j.jssc.2004.08.002

2. Experimental

Single crystals of $UCo_{0.5}Sb_2$ have been grown from molten Sb by the so-called self-flux method in a similar way to that applied earlier for the parent compound USb_2 by Henkie et al. [4]. Uranium (purity 99.9%), cobalt and antimony (purity 99.99%) were weighed in the atomic ratio of 1:1:12 and placed in an alumina crucible. Then, the crucible was sealed in an evacuated silica tube, heated up to 1150 °C and held at this temperature for 10 h followed by slow cooling (2–3 °C/h) down to 600 °C. Next, the ampoule was fast cooled to room temperature and the crucible was transferred to the silica tube, where an excess of Sb was removed by means of sublimation in high vacuum at 600 °C. For the purpose of homogenization, crystals were wrapped in Ta foil, sealed in an evacuated silica tube and annealed at 800–850 °C for two weeks. The obtained crystals were examined using an optical microscope and a scanning electron microscope (SEM) Philips 515. The phase composition was checked by powder X-ray diffraction (XRD) employing CoK_α radiation ($\lambda = 0.179021$ nm) The chemical composition was determined with an energy dispersive X-ray (EDX) spectrometer PV9800. The crystal structure was refined from the single-crystal X-ray diffraction data using Xcalibur-CCD diffractometer (MoK_α radiation—$\lambda = 0.071073$ nm). Intensity data were collected at room temperature with the ω scan mode and an exposure time per frame of 30 s. In the analysis an analytical absorption correction [5] has been applied. Magnetization measurements in magnetic fields up to 5 T were performed on oriented single crystals with a SQUID magnetometer (Quantum Design) in the temperature range 2–400 K.

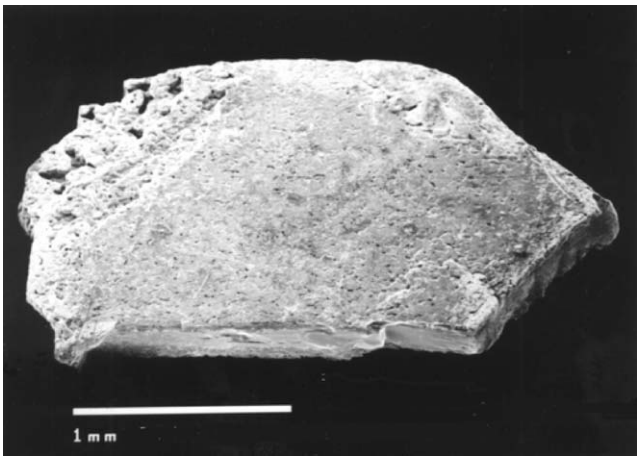

Fig. 1. The SEM image of a $UCo_{0.5}Sb_2$ single crystal.

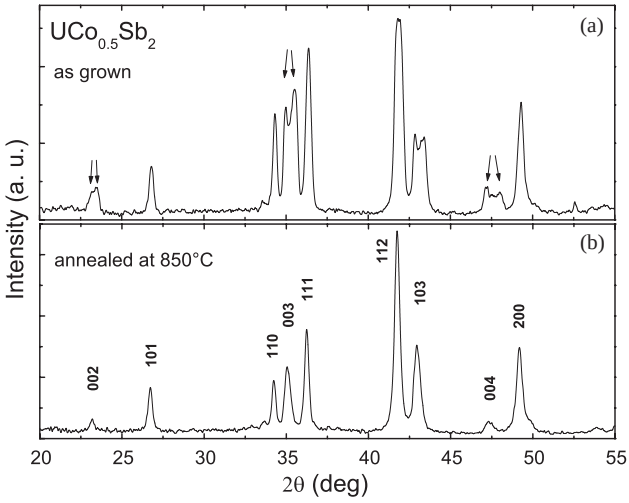

Fig. 2. The X-ray powder diffraction patterns for $UCo_{0.5}Sb_2$ crystals: (a) as grown, (b) after annealing in vacuum at 850 °C for 14 days. The arrows point to split reflections of the *00l*-type.

3. Results and discussion

3.1. Chemical composition

Single crystals of the title compound grew in the form of irregular platelets with the *c*-axis perpendicular to their surface with typical dimensions of $3 \times 5 \times 1\,mm^3$. The SEM image of the typical grown single crystal is shown in Fig. 1. Although the surface of the crystals was rather rough, their fracture possessed a metallic luster. The results of EDX analysis of the selected crystals (U, 29%; Co, 13%; Sb, 58%) indicated a significant deviation from the expected 1:1:2 stoichiometry yielding the chemical composition around $UCo_{0.5}Sb_2$. Except for the $UCo_{0.5}Sb_2$, in the same batch we have found also crystals of a nonmagnetic compound $CoSb_3$, which grew simultaneously. The latter crystals having a cubic structure were easy to distinguish and separate from the plate-like $UCo_{0.5}Sb_2$ ones. The presence of $CoSb_3$ crystals may be a further evidence that Co entered to the uranium-containing compound only partially.

Single crystals of $UCo_{0.5}Sb_2$ were stable in air over long period of time. This is in contrast to the parent compound, USb_2, which slowly oxidizes being exposed to air.

The X-ray powder diffraction pattern of crystals "as grown", shown in Fig. 2a, revealed a noticeable splitting of the *00l*-type reflections. All the observed diffraction lines could be indexed as belonging to the two phases with the same lattice parameter *a* (0.4298(1) nm) and distinctly different *c*-parameters i.e., 0.8826(2) and 0.8959(2) nm. This observation might be explained as a result of inhomogeneous distribution of Co-atoms in crystals during the process of growth. After the homogenizing annealing of crystals at 850 °C for 2 weeks the observed X-ray line splitting disappeared (see

Fig. 2b), confirming the homogeneity of our material. The X-ray powder diffraction pattern made on powdered crystals after annealing exhibited the absence of any unindexed reflections which may suggest that any impurity content in the sample does not exceed 3% (a detectability limit of the X-ray method). All the observed reflections could be easily indexed on the basis of a tetragonal cell, with the lattice parameters $a = 0.4299(1)$ and $c = 0.8924(2)$ nm. The lattice parameter c of $UCo_{0.5}Sb_2$ compared to that of the poly-crystalline $UCoSb_2$ sample ($c = 0.9075(4)$ nm) [1], is found to be substantially smaller. This is consistent with the incomplete occupation of the Co sites in the unit cell of this uranium ternary intermetallic compound.

It is worthwhile noting that such incomplete occupation of the transition metal positions has been observed for many isotypic $RTSb_2$ compounds (R = rare earth, T = Cu, Mn, Co, Cd, Fe, Zn). The magnitude of the deviation from the ideal stoichiometry and homogeneity ranges are somehow dependent on the transition element. This could be illustrated by the following series of the antimonides: $LaCu_{0.82-0.87}Sb_2$, $LaMn_{0.65-0.76}Sb_2$, $LaCo_{0.68}Sb_2$ [6], $LaCd_{0.7}Sb_2$ [7], $NdFe_{0.6}Sb_2$ [8], $LaZn_{0.52}Sb_2$ [6]. The deviation from the full occupancy of the transition metal sites is relatively small for R = Cu and increases across the series T = Mn, Co, Cd achieving the largest value for T = Fe, Zn. In contrast to the above compounds, $RAuSb_2$ [7] and $RAgSb_2$ [2,9,10] were found with fully occupied Au and Ag positions. Furthermore there are no reports on the deviation from perfect stoichiometry in $RTSb_2$ for heavier lanthanides (Tb-Lu). Our earlier report on $UNi_{0.5}Sb_2$ [3] and the results of this work suggest that the considerable deficiency on the transition metal sites is probably a common feature also for the remaining UT_xSb_2 compounds.

Table 1
Crystal data and structure refinement for $UCo_{0.5}Sb_2$

Crystal system, space group	tetragonal, $P4/nmm$
Unit cell dimensions	$a = 0.43000(10)$ nm
	$c = 0.8958(2)$ nm
Z, Calculated density	2, 10.246 Mg/m^3
Crystal dimensions	$0.1 \times 0.1 \times 0.03$ mm^3
Absorption coefficient	68.390 mm^{-1}
$F(0\,0\,0)$	415
Theta range for data collection	4.55–30.49°
Limiting indices	$-5 \leqslant h \leqslant 7$, $-6 \leqslant k \leqslant 5$, $-10 \leqslant l \leqslant 16$
Reflections collected/unique	2732/346 [R(int) = 0.1033]
Completeness to theta = 26.30	99.7%
Refinement method	Full-matrix least-squares on F^2
Data/restraints/parameters	346/0/16
Goodness-of-fit on F^2	1.050
Final R indices [$I > 2\sigma(I)$]	$R_1 = 0.0451$, w$R_2 = 0.1147$
R indices (all data)	$R_1 = 0.0496$, w$R_2 = 0.1188$
Extinction coefficient	0.014(4)
Largest diff. peak and hole	8.974 and −6.386 e.A^{-3}

3.2. Crystal structure

The crystal structure of $UCo_{0.5}Sb_2$ and anisotropic displacement parameters were successfully refined using a SHELXL-97 programm [11]. The starting atomic parameters were taken as those of the $RTSb_2$ compounds (R: rare-earth metals) [2]. The occupancy factors were refined in a separate series of least-squares cycles, giving no significant deviation from the full occupancies for uranium, and antimony, and a value of ~ 0.5 for cobalt atoms. The crystallographic and experimental details are summarized in Table 1. Occupancy factors, positional and anisotropic displacement parameters, are given in Table 2. It could be noticed that the displacement parameters for the Co atoms are considerably larger than those for the U and Sb atoms. This fact might suggest that the Co atoms are more mobile within their layers than the remaining atoms (Fig. 3).

In the case of $UCo_{0.5}Sb_2$, contrary to $UNi_{0.5}Sb_2$ [3], the reflections connected with a superstructure have not been detected.

3.3. Magnetic properties

Magnetization curves taken at 2 K, shown in Fig. 4, reveal a pronounced remanence and an almost rectangular hysteresis loop for $M^{\parallel}(B)$. This behavior is typical for the hard ferromagnetic materials. As Fig. 4 indicates, the virgin magnetization curve has initially (up to 1.5 T) negligible magnetic response ascribed to the domain-wall pinning effect. In fields above 5 T, the saturation of

Table 2
Atomic coordinates, equivalent isotropic and anisotropic displacement parameters (nm$^2 \times 10^4$) for $UCo_{0.5}Sb_2$

Atoms	Occupation	x	y	z	U_{eq}	U_{11}	U_{22}	U_{33}
U	1.01(9)	1/4	1/4	0.2754(1)	0.9(1)	0.9(1)	0.9(1)	0.9(1)
Sb(1)	1.00(9)	3/4	1/4	0	0.9(1)	0.9(1)	0.9(1)	0.7(1)
Sb(2)	0.97(9)	1/4	1/4	0.6377(1)	1.0(1)	1.0(1)	1.0(1)	1.0(1)
Co	0.46(4)	3/4	1/4	1/2	2.8(7)	2.4(9)	2.4(9)	3.6(12)

$U_{23} = U_{13} = U_{12} = 0$

The U_{eq} is defined as one third of the trace of the orthogonalized U_{ij} tensor. The anisotropic displacement factor exponent takes the form: $-2\pi^2[h^2a^{*2}U_{11} + \cdots + 2hka^*b^*U_{12}]$.

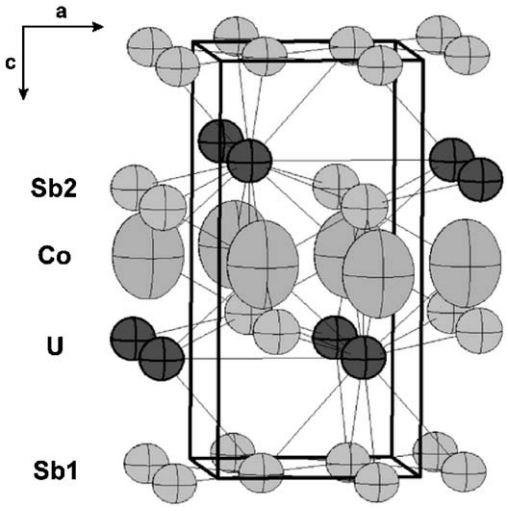

Fig. 3. Three-dimensional representation of the $UCo_{0.5}Sb_2$ unit cell.

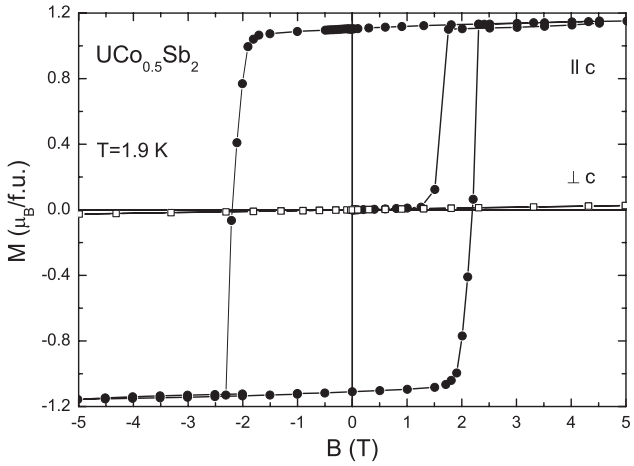

Fig. 4. Magnetization of $UCo_{0.5}Sb_2$ as a function of applied magnetic field.

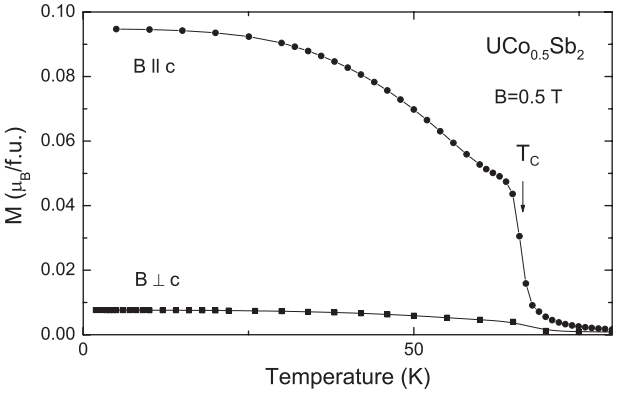

Fig. 5. Magnetization of $UCo_{0.5}Sb_2$ as a function of temperature.

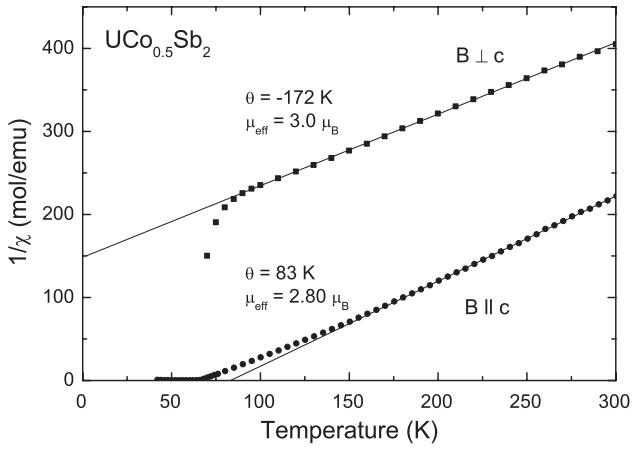

Fig. 6. Reciprocal magnetic susceptibility vs. temperature for $UCo_{0.5}Sb_2$.

the magnetization becomes almost completed, yielding a saturation moment of $1.2\,\mu_B$/at.U. In turn, the magnetization in the *ab*-plane is very small and almost linear in a magnetic field. Thus, it becomes clear that the *c*-axis is equivalent with an easy magnetization axis. Fig. 5 shows the temperature dependence of the magnetization measured in a magnetic field of 0.5 T. From this dependence $T_C = 65\,\mathrm{K}$ is inferred. As is furthermore demonstrated, the magnetization in the basal plane below T_C is much smaller than that along the *c*-axis. The inverse magnetic susceptibility measured perpendicular to the *c*-axis, $\chi_\perp^{-1}$, and along the *c*-axis, $\chi_\parallel^{-1}$, is displayed in Fig. 6. As seen, both the susceptibilities can be fitted to the Curie–Weiss law: $\chi(T) = C/(T - \Theta_p)$, where $C = \mu_0 N_A \mu_{\mathrm{eff}}^2/3k_B$ at temperatures above 150 and 100 K, respectively. This yields the effective magnetic moment μ_{eff} of approximately $3\,\mu_B$/at.U for both crystal orientations. On the other hand, the paramagnetic Curie temperature determined along the *ab*-plane ($\Theta_p^\perp = -172\,\mathrm{K}$) and along the *c*-axis($\Theta_p^\parallel = 83\,\mathrm{K}$) are substantially different in their magnitude and sign. This indicates a huge magnetocrystalline anisotropy existing in this compound. Usually, the difference $\Delta\Theta_p = \Theta_p^\parallel - \Theta_p^\perp$, accounting here to 255 K, may be regarded as a measure of uniaxial magnetic anisotropy energy. To identify the origin of the observed anisotropy it is worthwhile mentioning the value of magnetocrystalline anisotropy found in isostructural $RTSb_2$ compounds [12]. The average difference $\Delta\Theta_p$ of the order of 70 K, determined for the latter compounds, has been explained in Ref. [12] on a basis of the crystal electric field effect (CEF) model only. By comparison one sees, that the difference $\Delta\Theta_p = 255\,\mathrm{K}$ observed here in $UCo_{0.5}Sb_2$ is relatively large and may have except CEF effect also a different origin. We suppose that apart from CEF, the contribution from an anisotropic hybridization between the 5*f*-electrons and electrons of ligands plays here an equally important role.

4. Conclusions

We have successfully grown good quality single crystals of the Co-containing uranium diantimonide $UCo_{0.5}Sb_2$ by means of the antimony flux technique. This compound crystallizes in the same crystal structure as the other $UTSb_2$ do, i.e., in the tetragonal $HfCuSi_2$-type. The refinements of the occupancy parameters and EDX analysis indicated a substantial deficiency on the cobalt sites suggesting $UCo_{0.5}Sb_2$ composition. We have shown that this compound orders ferromagnetically below 65 K and exhibits a high magnetocrystalline anisotropy with the *c*-axis as the easy magnetization direction. The giant magnetocrystalline anisotropy observed in $UCo_{0.5}Sb_2$ is supposed to originate not only from the CEF effect but very likely also from an anisotropic 5*f*-ligand hybridization effect.

Acknowledgments

The authors wish to thank E. Bukowska for performing powder X-ray diffraction patterns, K. Nierzewski for SEM/EDX analyses and R. Gorzelniak for collecting magnetization data. Financial support from KBN Grant No 2 PO3B 109 24 is acknowledged.

References

[1] D. Kaczorowski, R. Kruk, J.P. Sanchez, B. Malaman, F. Wastin, Phys. Rev. B 58 (1998) 9227.
[2] M. Brylak, M.H. Möller, W. Jeitschko, J. Solid State Chem. 115 (1995) 305.
[3] Z. Bukowski, D. Kaczorowski, J. Stepień-Damm, D. Badurski, R. Troć, Intermetallics, in press.
[4] Z. Henkie, A. Misiuk, Kristall Technik 14 (1978) 539.
[5] CrysalisRED. Version 1.71, Oxford, 2003.
[6] G. Cordier, H. Schäfer, P. Woll, Z. Naturforsch. B 40 (1985) 1097.
[7] P. Wollesen, W. Jeitschko, M. Brylak, L. Dietrich, J. Alloys Compd. 245 (1996) L5.
[8] A. Leithe-Jasper, P. Rogl, J. Alloys Compd. 203 (1994) 133.
[9] O. Sologub, H. Noël, A. Leithe-Jasper, O.I. Bodak, J. Solid State Chem. 115 (1995) 441.
[10] L. Zeng, X. Xie, H.F. Franzen, J. Alloys Compd. 343 (2002) 122.
[11] G.M. Sheldrick, Program for Crystal Structure Refinement, University of Göttingen, Germany, 1997.
[12] A. Thamizhavel, T. Takeuchi, T. Okubo, M. Yamada, R. Asai, S. Kirita, A. Galatanu, E. Yamamoto, T. Ebihara, Y. Inada, R. Settai, Y. Onuki, Phys. Rev. B 68 (2003) 54427.